参赛队员姓名：耿佳滢 Jiaying Geng

中学：Dulwich College Beijing

省份：北京

国家/地区：中国

指导教师姓名：Feng Tian

指导教师单位：Beth Israel Deaconess Medical Center / Harvard Medical School

论文题目：Molecular examination of the possibility for ALS Reversals and Plateaus

Molecular examination of the possibility for ALS Reversals and Plateaus

Jiaying Geng

Abstract

Amyotrophic Lateral Sclerosis (ALS) is a devastating neurodegenerative disease caused by the loss of motor neurons (MN) across the brain and spinal cord. Despite its aggressive nature, a small fraction of ALS patients exhibit reversals and plateaus, where the disease's progression temporarily halts or even reverses, leading to notable recovery of motor functions. In this study, I examined the molecular mechanisms underlying "ALS Reversals" by performing cell-type characterization and ALS Reversal gene screening on single-nuclei and single-cell RNA sequencing data. To test my hypothesis, I studied the effects of upregulating ALS Reversal-associated pathways on the longevity and behavior of an ALS animal model of *Caenorhabditis elegans* (*C. elegans*). The results of this study not only revealed two surprising cell-specific pathways implicated in ALS Reversals but also showcased their combined synergistic potential in augmenting neuroprotective effects, as evidenced by improved lifespan and motor function in worm ALS models. This study may pave the way for a deeper understanding of ALS Reversals mechanisms, and inspire new directions for therapeutic interventions in ALS.

Keywords: Amyotrophic Lateral Sclerosis; Single-cell RNA sequencing; Alpha Motor Neurons; Machine Learning; Bioinformatics; Multiple Sclerosis

Table of Contents

Abstract **2**

1. Introduction **4**

1.1. Scientific Background 4

1.2. Research Question 5

1.3. Significance and Innovation 6

2. Methods **6**

2.1. Computational Analysis of Spinal Cord single-nuclei and Multiple Sclerosis single-cell RNA sequencing datasets (Dry Lab) 7

2.1.1. Spinal Cord Nuclei Dataset Selection and Pre-Processing 7

2.1.2. Clustering and Cell-Type Identification using Machine Learning 7

2.1.3. Sub-clustering and MN Subtype Identification using Machine Learning 7

2.1.4. Multiple Sclerosis Oligodendrocyte Data Selection, Pre-Processing and Clustering using Machine Learning 8

2.2. *C. elegans* Experimental Procedure (Wet lab) 8

2.2.1. Nematode Strain maintenance and treatment 8

2.2.2. Preparation of Treatment Solutions and Concentrations 8

2.2.3. Experimental Methods 9

2.2.4. Lifespan Assay 9

2.2.5. Behavioral Assay 9

2.2.6. Statistical Analysis 9

3. Results **10**

3.1. Motor Neuron Subtype Analysis of ALS Reversal-associated Genes Reveals gene expression patterns 10

3.1.1. Screening ALS Reversal-associated genes across MNs 10

3.1.2. Screening ALS Reversal-associated genes across Susceptible Motor Neuron Subtypes 12

3.2. Gene Analysis of Remyelinated MS ODC Dataset reveals ALS Reversal-associated Gene involvement in ODC wound regeneration and myelination 14

3.3. Effect of ALS Reversal pathway-inducing medication on C. elegans 17

3.3.1. Combinatorial Treatment of Trehalose & MK677 extends lifespan in SOD1 worm models 18

3.3.2. Combinatorial Treatment alleviates motor dysfunction in SOD1 worm models 19

4. Discussion **22**

References **24**

Acknowledgements **27**

Declaration of Academic integrity **27**

Supplementary Data **28**

1. Introduction

1.1. Scientific Background

Amyotrophic Lateral Sclerosis (ALS), also known as Lou Gehrig's disease, is a devastating neurodegenerative disease characterized by the selective degeneration and death of motor neurons (MNs). Pathological symptoms of ALS include the denervation of voluntary muscles, muscle atrophy, MN demyelination, and corticobulbar onset (**Fig. 1**) [1]. The prevalence of ALS is approximately 6 per 100,000 individuals worldwide [2], and projected to increase 69% by the year 2040 [3]. The mean survival time of patients after symptom onset is 2–4 years, and patient death is often due to respiratory failure [4].

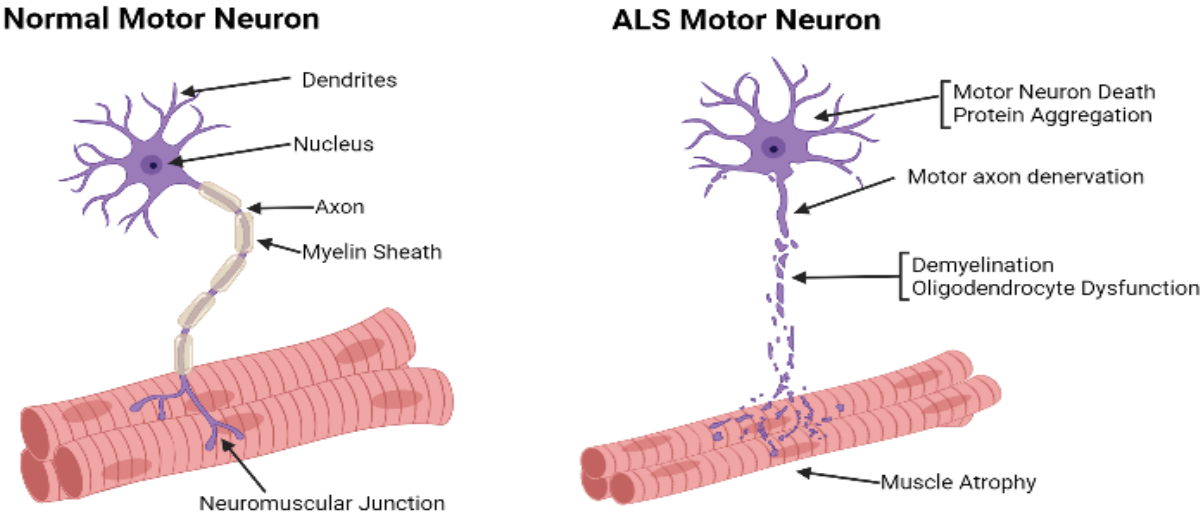

Fig. 1 Representation of healthy and ALS affected motor neurons. Created with Biorender.com.

Unfortunately, there is currently no disease modifying drug for ALS. A variety of FDA-Approved ALS drug treatments are available, but only slow disease progression and prolong patient lifespan by a few months. Current ALS drugs include Riluzole, which inhibits glutamate release [5], AMX0035, which slows MN cell death by targeting MN ER and mitochondria [6], and Edaravone, an antioxidant that combats oxidative stress in ALS pathogenesis. Due to the lack of adequate treatment options, it is commonly recognized that ALS progression is both rapid and irreversible. However, a small portion of ALS patients seem to experience a plateau or even show recovery of lost functions after the onset of the disease. For instance, some patients regain bulbar abilities that they had previously lost during the progression of the disease [7]. A few studies sought to carefully define the plateau and potential reversals of ALS. "ALS Reversals" are characterized by three criteria: (1) clinically diagnosed ALS patients

experiencing (2) consistent symptom onset [8] and (3) dramatic and sustained recovery by multiple measures, such as ALSFRS-R (ALS Functional Rating Scale – Revised) [9].

ALS Reversals are still a topic of ongoing debate, as many questions of ALS reversal research are yet to be answered. Two main problems remain unanswered in this field of ALS research: Firstly, only 48 ALS reversal patients have been identified [10]. This small sample size of ALS patients limits the accuracy and credibility of any analysis done on these patients. Secondly, whole genome sequencing of these ALS Reversal patients is currently underway [11]. To date, two ALS Reversal-associated genes have been identified: Syntaxin Binding Protein 6 (STXBP6) and Insulin-like growth factor binding protein 7 (IGFBP7) [12]. However, the identification of these genes does not elucidate the mechanisms underlying ALS Reversals. It remains unclear whether ALS MN degeneration can be reversed at a molecular level.

1.2. Research Question

My research to uncover potential cellular pathways of ALS Reversals and plateaus is guided by three questions: 1) Can ALS Reversals related genes be validated at a molecular level? 2) Are there diseases of similar pathological features to ALS that exhibit larger populations in functional plateaus, and if so, can we draw parallels between its recovery mechanisms and ALS reversal's pathways? 3) Can the novel molecular pathways of ALS Reversals provide insight to future therapeutic directions of ALS?

To address these questions, I employ machine learning algorithms to perform single-nuclei sequencing (snRNA-seq) to validate ALS Reversals, and determine cell-specific molecular pathways of ALS plateaus and reversals. Moreover, I investigate if the functions of ALS Reversal-associated genes overlap with those of ALS-associated genes. Secondly, I compare ALS with a disease with shared pathological features but more populations in functional remissions. For this purpose, I have chosen Multiple Sclerosis (MS), a neurodegenerative disease characterized by central nervous system (CNS) lesions. A major pathological feature of MS, demyelination of oligodendrocytes in the CNS, causes progressive debilitating illness. Similarly, dysfunction of oligodendrocytes and demyelination in ALS are suggested to contribute to the progression of ALS pathogenesis [13]. However, some populations of MS patients show remyelination of neurons, leading to halting of symptom pathogenesis, and even functional recovery in rare cases [14]. These disease phenotypes are largely similar to those demonstrated by ALS reversal patients. Thus, I use machine learning tools to analyze single cell sequencing (scRNA-seq) data to analyze parallels between cell-type specific mechanisms of recovery for both MS remyelination and ALS Reversals, uncovering molecular pathways

for mechanisms underlying ALS functional plateaus and reversals. Finally, I suggest potential therapeutic treatments for ALS by testing my ALS Reversal mechanism hypothesis, examining effect of upregulating ALS Reversal-associated pathways on ALS-related mutant human SOD1 (hSOD1) transgenic *Caenorhabditis elegans* (*C. elegans*).

1.3. Significance and Innovation

Due to the rarity of ALS Reversal cases, few studies have examined the possibilities and mechanisms of Reversals at a molecular level. Thus, by employing machine learning-based algorithms and wet lab procedures to characterize ALS Reversal-related genes, this paper aims to uncover novel mechanisms underlying these miraculous ALS recoveries. Better understanding of ALS Reversals could shed light on more strategies to develop effective ALS therapeutics and recreate functional recoveries on larger ALS patient populations.

2. Methods

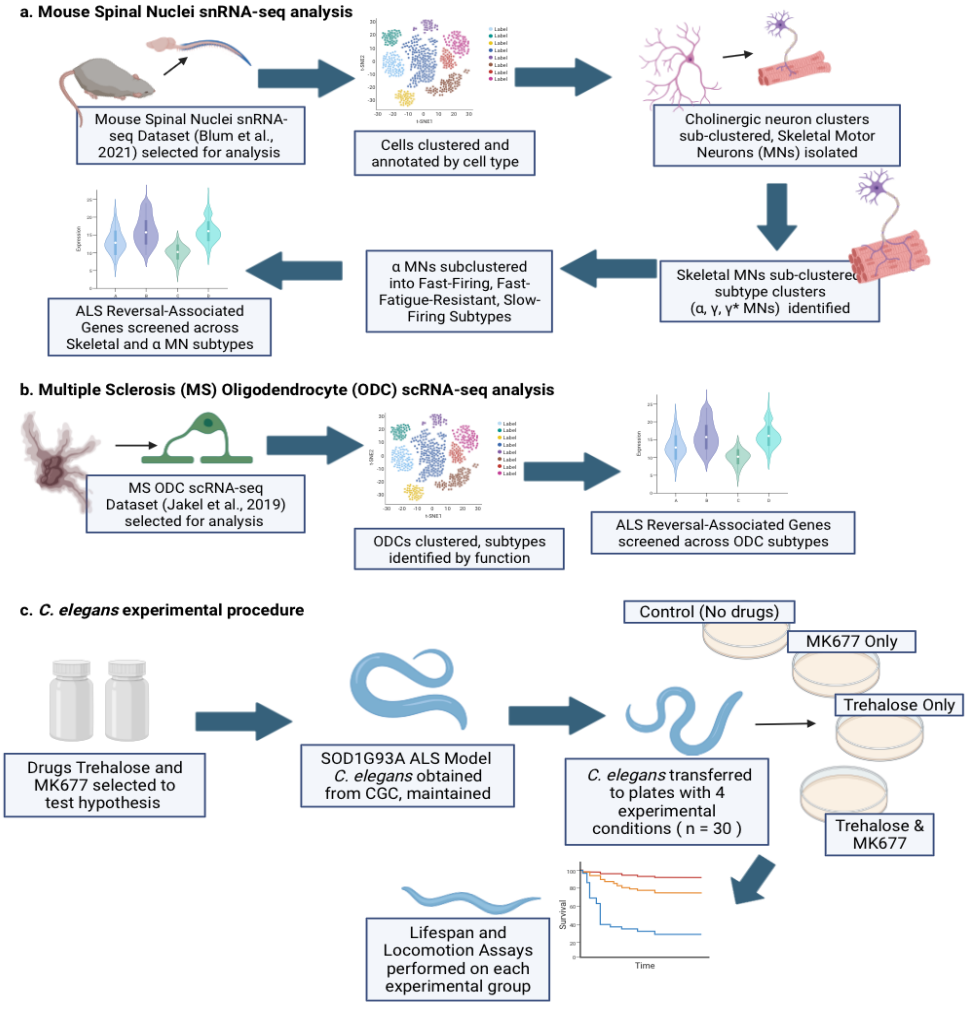

Fig. 2 Flowchart of computational analysis and wet lab procedure. Created with Biorender.com.

2.1. Computational Analysis of Spinal Cord single-nuclei and Multiple Sclerosis single-cell RNA sequencing datasets (Dry Lab)

2.1.1. Spinal Cord Nuclei Dataset Selection and Pre-Processing

Data was obtained from a study conducted by Blum et al. [15], a snRNA-seq dataset collecting spinal cord nuclei from mice models. The dataset, which comprises data from 43,890 nuclei, is comprehensive and provides a solid foundation for gene expression analysis. Wild-type mice were dissected and their spinal cords extracted for snRNA-seq, and the dataset obtained was deposited in the Gene Expression Omnibus (GEO) under the access code GSE161621.

I performed subsequent snRNA-seq data analysis on the dataset using the Seurat v4.3.0 [16], an R Package commonly used to analyze scRNA-seq and snRNA-seq data. The dataset was pre-processed through standard procedures and functions. Quality control on the nuclei was performed, followed by data normalization using the "NormalizeData" function, and highly variable genes were selected for downstream analysis and clustering using the "FindVariableFeatures" function.

I reduced data dimensionality using the principal component analysis (PCA) [17], a technique that uses variable genes to determine expression variance. The top 30 principal components were used for subsequent downstream analysis.

2.1.2. Clustering and Cell-Type Identification using Machine Learning

Next, I reproduced the clusters of cell types as identified in the original study by Blum et al. using machine learning. Cells were clustered using the "FindNeighbors" and "FindClusters" functions. Both of these are unsupervised machine learning techniques based on the Louvain algorithm [18], which groups neighboring communities. This generated 38 clusters, each cluster corresponding to the 38 clusters generated in the original study. These clusters were visualized using the uniform manifold approximation and projection (UMAP) technique, as shown in Supplementary Figure 1. UMAP is an unsupervised machine learning tool that aids in visualizing dimensional reduction [19]. For identifying cell types within these clusters, I utilized a manually curated list of canonical markers, as provided in the original study.

2.1.3. Sub-clustering and MN Subtype Identification using Machine Learning

I reproduced the subtypes of MN cell types as identified in the original study. Cholinergic neuron clusters were isolated and further sub clustered using the unsupervised machine learning functions, "FindNeighbors" and "FindClusters", generating 11 clusters matched with

the original study. MN clusters were identified and isolated from the Cholinergic neuron clusters, further clustered using unsupervised learning function “FindNeighbors” and “FindClusters”, and annotated by MN subtypes using a manually curated list of canonical markers from the original study.

2.1.4. Multiple Sclerosis Oligodendrocyte Data Selection, Pre-Processing and Clustering using Machine Learning

Multiple Sclerosis data was obtained from a study by Jakel et al. [20], a large scRNA-seq dataset collecting white matter containing oligodendrocytes from post mortem tissue of four human controls and five MS patients. This dataset was chosen because it contained remyelinated MS cells, making it valuable for genetic mechanism analysis of MS functional recoveries. The dataset obtained was deposited in the Gene Expression Omnibus (GEO) under the access code GSE118257. Pre-processing steps identical to the quality control, normalization and dimensionality reduction procedures done in 2.1 were performed on this dataset.

After pre-processing, Remyelinated and Demyelinated MS Oligodendrocytes were identified from the original dataset and each clustered using the unsupervised learning functions “FindNeighbors” and “FindClusters”.

2.2. *C. elegans* Experimental Procedure (Wet lab)

2.2.1. Nematode Strain maintenance and treatment

ALS-related SOD1 G93A(rt449[G85RC]) *C. elegans* strain was provided by the *Caenorhabditis* Genetics Center (University of Minnesota, Minneapolis, MN). This transgenic worm strain models the symptom and disease progression of ALS SOD1 human patients, making it a useful tool for studying the effect of pathway upregulation on ALS pathogenesis. Worms were grown on nematode growth medium (NGM) plates seeded with 150 μl spots of E. *coli* (strain OP50) as a food source. For age synchronization, hermaphrodite nematodes were transferred to NGM plates at L4 stage of development and allowed to lay eggs overnight. L1 hatchlings were isolated and cultured on fresh NGM plates at 25 ℃. Once age-synchronized hatchlings reached stage L4, experimental group worms were transferred to plates containing drugs.

2.2.2. Preparation of Treatment Solutions and Concentrations

Trehalose was dissolved in sterile water to prepare a 300x stock solution, which was added to cooled (50 ℃) NGM liquid at a concentration of 5 mM to create fresh NGM plates containing

only trehalose. MK677 was dissolved in sterile water to prepare a stock solution, and later added to cooled NGM liquid at a concentration of 16 μM to create fresh plates containing only MK677. NGM plates containing both MK677 and Trehalose contained a concentration of both 5mM Trehalose and 16 μM MK677. Age-synchronized worms were transferred to fresh NGM plates once they reached L4 stage.

2.2.3. Experimental Methods

120 hermaphrodite, age-synchronized L4 (day 3.5) ALS-related SOD1 G93A C. *elegans* were randomly split into 4 experimental groups: one control group (n = 30), one group with only Trehalose (Sigma-Aldrich) administered (n = 30) as a positive control, one group with only MK677 (Sigma-Aldrich) administered (n = 30), and one group with both Trehalose and MK677 administered (n = 30). Drugs were administered into fresh NGM plates and fed to worms at stage L4. Immediately after transference of worms, lifespan assays were performed on each group, while locomotion assays were performed on day 7, 9 and 11.

2.2.4. Lifespan Assay

Lifespan assays were performed according to established protocols [21]. Briefly, Age-synchronized L4 stage worms were transferred to OP50 seeded NGM plates with different drug conditions. The next day was defined as day 1. Worm viability is measured each day; worms exhibiting no swallowing or movement when gently or harshly touched with a pick are scored as dead. Lifespan are scored each day until all animals are dead. Survival curves were analyzed by GraphPad Prism (GraphPad, La Jolla, CA, USA, ver. 10.1).

2.2.5. Behavioral Assay

Worm locomotion is monitored according to previously described methods [22], with a few minor modifications. At day 7, one representative worm from each experimental condition were individually transferred to a freshly seeded, non-drug NGM plate, and their crawling behavior was recorded for 50s. The video was collected, and the relative movement, calculated by the ratio of movement distance to body length, was measured by Image J. This procedure was repeated on day 9 and day 11 to gain an elapsed view of motor function degeneration throughout worm lifespan. A total of 12 videos were collected across these three independent days.

2.2.6. Statistical Analysis

Data were analyzed using Graphpad Prism software (ver. 10.0.1). Lifespan between experimental conditions were analyzed by Kaplan-Meier survival analysis. Differences

between experimental groups were evaluated with the unpaired *t*-test (2-tailed): ***P < 0.0001; **P < 0.001; *P < 0.05. Lifespan data significance was evaluated through the Log-rank (Mantel-Cox) test. P < 0.05 was considered statistically significant.

3. Results

3.1. Motor Neuron Subtype Analysis of ALS Reversal-associated Genes Reveals gene expression patterns

3.1.1. Screening ALS Reversal-associated genes across MNs

To characterize MN clusters from mouse nuclei, I clustered and reproduced seven cell types from spinal cord nuclei: Astrocytes, Cholinergic Neurons, Endothelial Cells, Excitatory interneurons, Inhibitory interneurons, Microglia/Macrophages and Oligodendrocytes. A heat map of canonical marker gene expression levels across seven cell types were generated (**Fig. 3**), and a UMAP visualizing the distinct cellular identity of each cluster (**Fig.4**). Consistently, the heatmap and UMAP analysis identify the same cell types (and subtypes) revealed by the original published dataset [15], which provides a molecular basis for the bioinformatic analysis described in later sections.

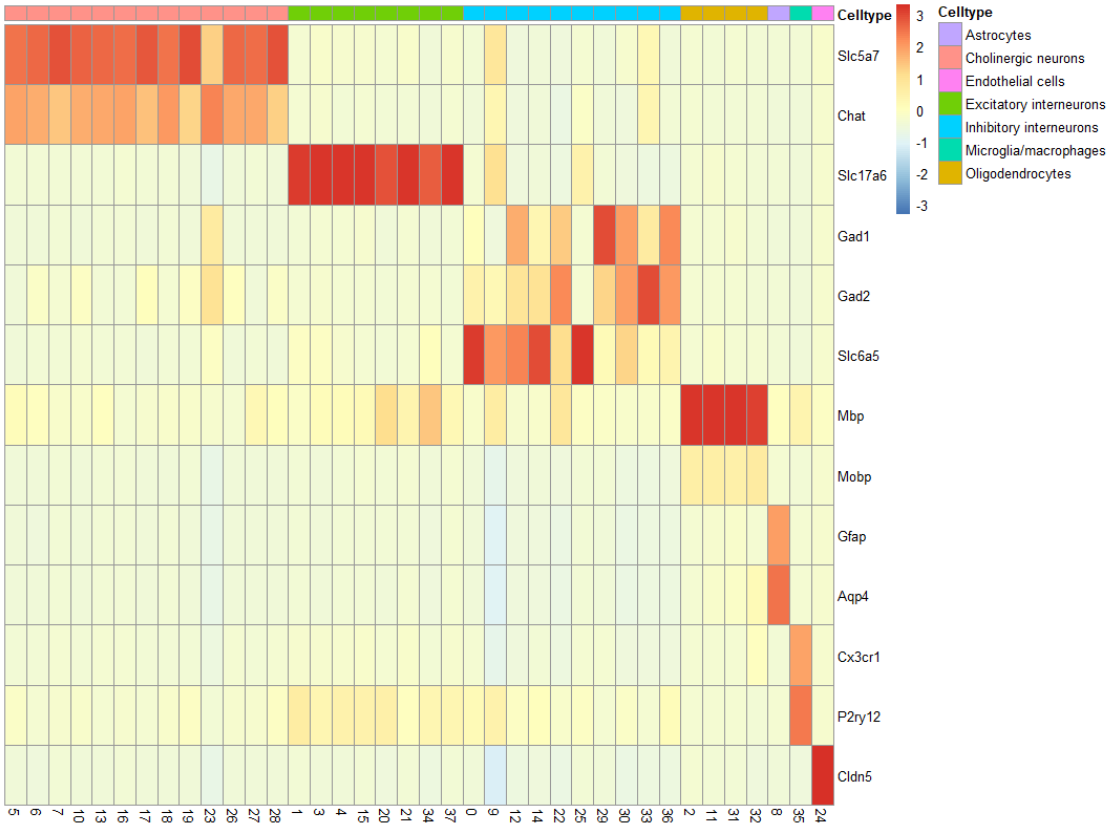

Fig. 3 Heatmap depicting average expression levels per cluster for marker genes of each cell type

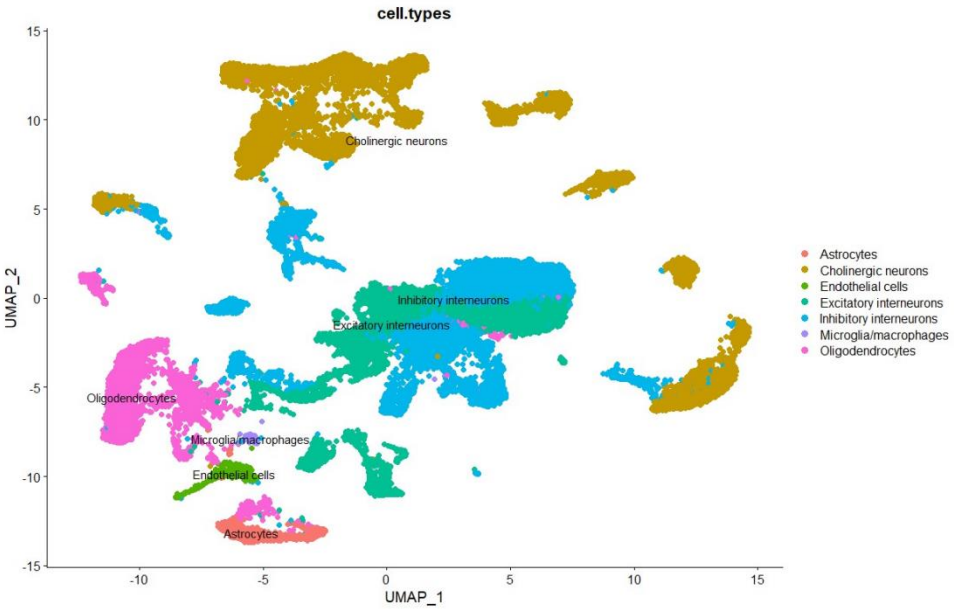

Fig. 4 Cell Clusters with assigned identities visualized using UMAP

I isolated Cholinergic neuron clusters for further analysis. Cholinergic neurons contain skeletal MNs, which include three prominent subtypes of Alpha (α), Gamma (γ) and Beta (Gamma Star / γ*) MNs. These MN subtypes are significant to ALS research, as they have vastly different susceptibilities to ALS: α MN selectively degenerate while γ MNs are spared in ALS pathogenesis [23]. The susceptibility of γ* MNs in ALS is unknown, as few studies have investigated the susceptibility of γ*MNs in ALS patients. I clustered and identified these three MN subtypes, and average expression of marker genes in α, γ and γ* MNs were overlaid on UMAP (**Fig. 5**), showing distinct identities for each of the clusters.

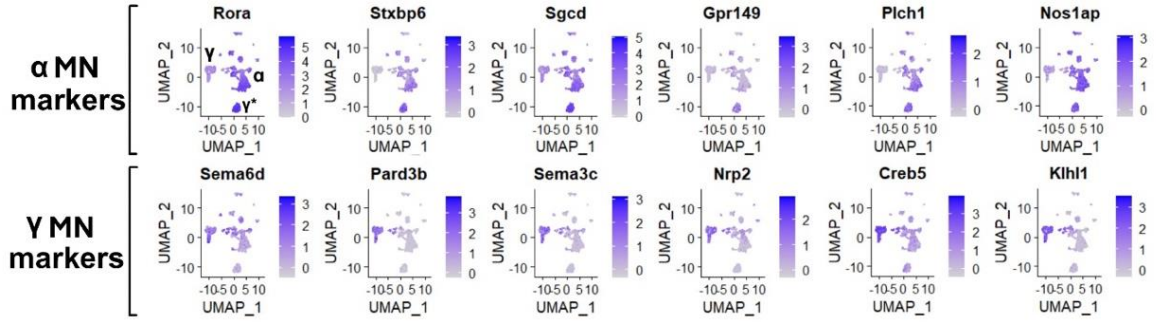

Fig. 5 UMAP representing clusters for α, γ and γ* MNs

After determining MN subtype identities, I visualized the expression of ALS Reversal-associated genes STXBP6 and IGFBP7 across MN subtypes in violin plots (**Fig. 6**). α and γ*MNs expressed an elevated expression of STXBP6, while all MN subtypes showed low expressions of IGFBP7. Since the gene IGFBP7 is minimally expressed in MN cell types, it may contribute to ALS Reversal pathways in other cell identities.

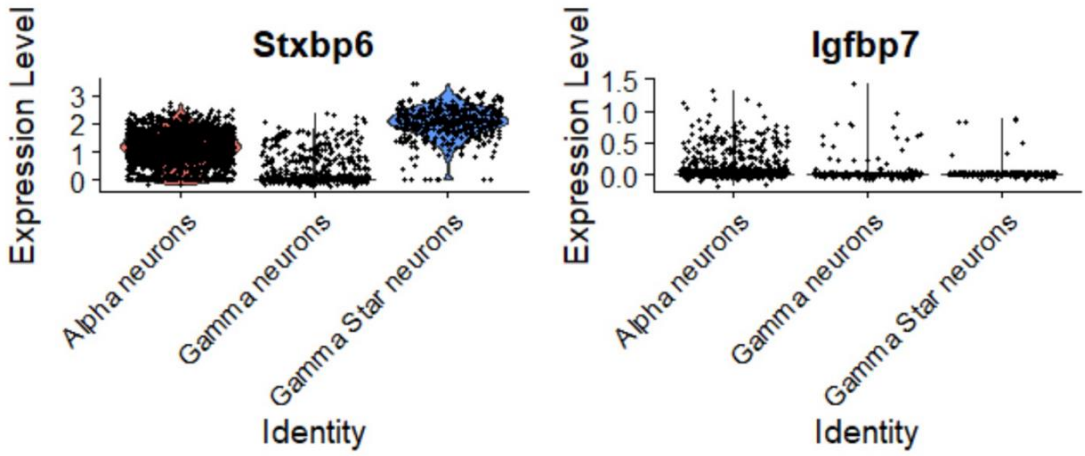

Fig. 6 Expression Pattern of ALS Reversal-associated genes visualized by Violin Plots

Notably, there is a high expression of STXBP6 in γ* MNs, the most elusive subgroup in the three MN subtypes. As no studies have examined γ* MN susceptibility to ALS pathogenesis, I will not be examining ALS Reversal involvement in γ* MNs in further detail. Instead, I will be focusing on the two other skeletal MN subtypes with known ALS susceptibilities (γ and α MNs) for further screening and analysis. However, this is an interesting result, as elevated expression levels of ALS Reversal genes may indicate γ* MN involvement in ALS symptom rescue. Future studies may explore the implications of targeting these MN subtypes in ALS therapies.

3.1.2. Screening ALS Reversal-associated genes across Susceptible Motor Neuron Subtypes

Next, I subclustered α MNs into subtypes for further gene screening and analysis. α MNs subtypes are especially important for molecular analysis of ALS Reversals, as the susceptibilities of ALS varies between these subtypes. α MNs can be subdivided into Fast-Firing and Slow-Firing (SF) MNs according to their contracting properties [15]. Fast-Firing MNs can be further categorized into Fast-Firing Fatigable (FF) and Fast-Firing Fatigue-Resistant (FR) types, identified by how long they continue the contraction. FF MNs are most susceptible to degeneration and denervation, followed by FR MNs. SF MNs are the most resistant to ALS, and degenerate the slowest [23].

To reproduce α MN subtypes, single cells from α MNs clusters were annotated and categorized into FF, FR and SF MNs using a manually curated list of canonical markers provided by the original study, and a heat map is generated showing differentially expressed marker genes of all alpha MNs (**Supplementary Fig. 1**).

I visualized the expression of ALS Reversal-associated genes STXBP6 and IGFBP7 across α MNs subtypes in violin plots (**Fig. 7**). Overall, STXBP6 is expressed more across all α MN subtypes than IGFBP7. Interestingly, SF MNs express elevated levels of STXBP6 relative to FF MNs, indicating a strong association between SF α MNs and ALS Reversals. This is especially exciting, as SF MNs are least susceptible to ALS. Hence, I hypothesized that elevated levels of STXBP6 in SF MNs may exert a neuroprotective effect of STXBP6 on MN survival.

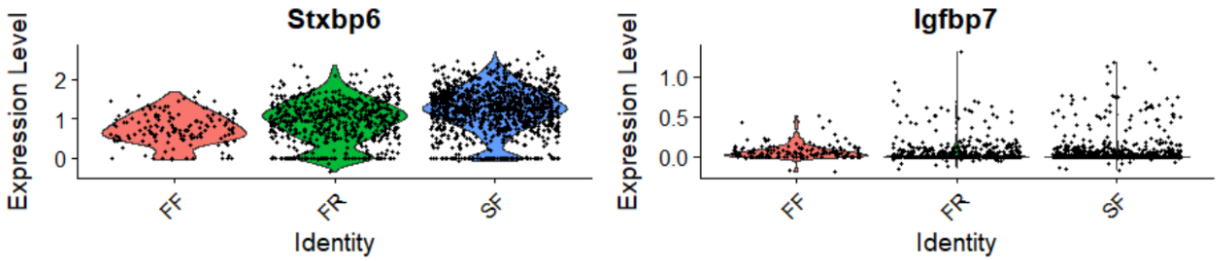

Fig. 7 Expression Pattern of ALS Reversal-associated genes in α MN subtypes visualized by Violin Plots

I investigated the specific molecular pathway STXBP6 acts to rescue ALS symptoms. STXBP6 is implicated in the generation of the SNARE complex within autophagy pathways, since prior research has shown that its over-expression induces autophagy [24]. Autophagy dysfunction has been theorized as a main cause of ALS pathogenesis [25]: it is plausible that accumulation of misfolded proteins commonly seen in ALS progression is caused by dysfunctional autophagy mechanisms, which may be a crucial factor causing MN death in the later stages of disease [26]. Hence, as implicated by the involvement of STXBP6 in autophagy induction, ALS Reversal patients may express more potent autophagy pathways, resulting in less autophagy dysfunction, decreased protein accumulation and notable recovery of movement abilities in later stages of pathogenesis.

To examine autophagy activity in α MNs, I found 18 genes associated with autophagy induction from previous literature [27]. I visualized the expression of these autophagy related genes across α MNs subtypes in violin plots (**Supplementary Fig. 2**). Of these 18 genes, ATG10, BCL2, ULK2, NBR1, OPTN and ATG16L1 follow the expression trends demonstrated by STXBP6 across α MNs, showing elevated expression particularly in SF MNs. (**Fig. 8**) These results indicate an elevated autophagy pathway is present in SF MNs, supporting STXBP6's hypothesized role in upregulating autophagy processes. It is possible that autophagy exerts a neuroprotective effect on SF MNs, contributing to their marked resistance against ALS pathogenesis. Hence, it can also be hypothesized that ALS Reversal patients have higher

activities of STXBP6-induced autophagy across MNs, which protects Reversal patients from MN degeneration and protein aggregation, allowing for functional recovery in later stages of disease progression.

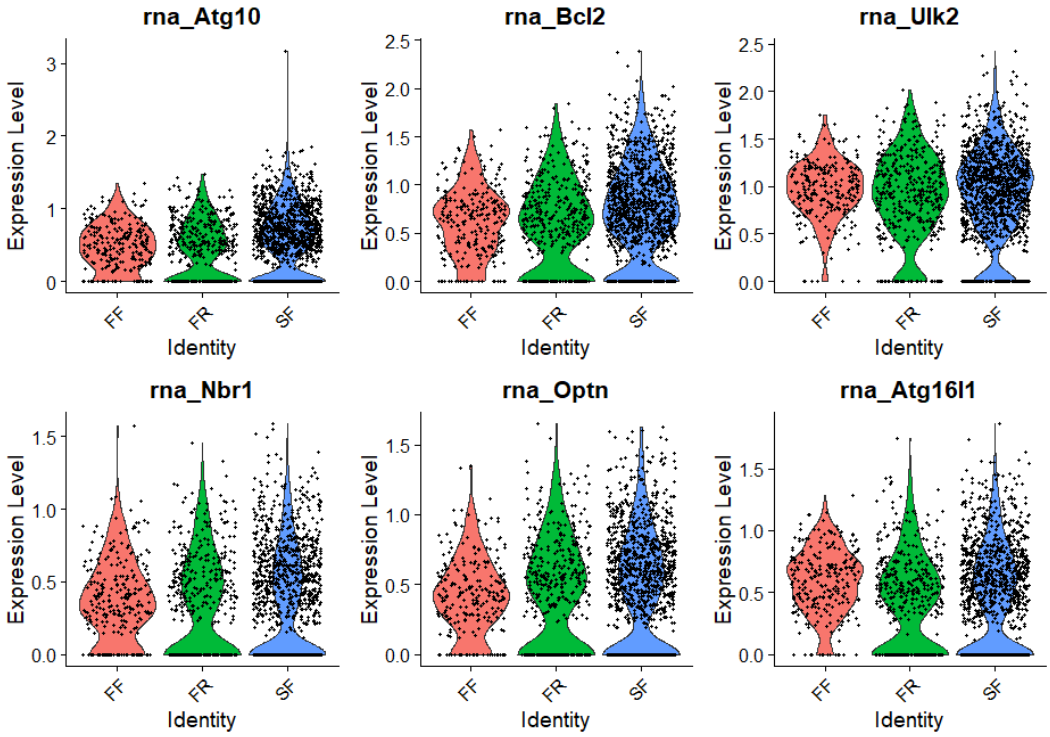

Fig. 8 Expression Pattern of Autophagy-associated genes across α MN subtypes

3.2. Gene Analysis of Remyelinated MS ODC Dataset reveals ALS Reversal-associated Gene involvement in ODC wound regeneration and myelination

Another molecular approach to complement examination of ALS Reversal pathways in mouse nuclei is to compare ALS with other pathologically similar neuron diseases. There are many shared pathological features, such as oligodendrocyte dysfunction, demyelination, between Multiple Sclerosis (MS) and ALS [28]. Thus, studying pathways underlying the remyelination mechanisms of MS can provide foundations for uncovering ALS Reversal and plateau mechanisms.

I isolated and pre-processed remyelinated MS oligodendrocytes in Jakel et al's scRNA MS dataset, and described in the methods section. Remyelinated MS ODCs clusters are relevant to my research, as they provide valuable insights to the molecular identity of functional plateaus and recoveries in MS patients. I clustered the remyelinated ODCs into 4 clusters. I visualized

the expression of ALS Reversal-associated genes across all remyelinated clusters in violin plots (**Fig. 9**).

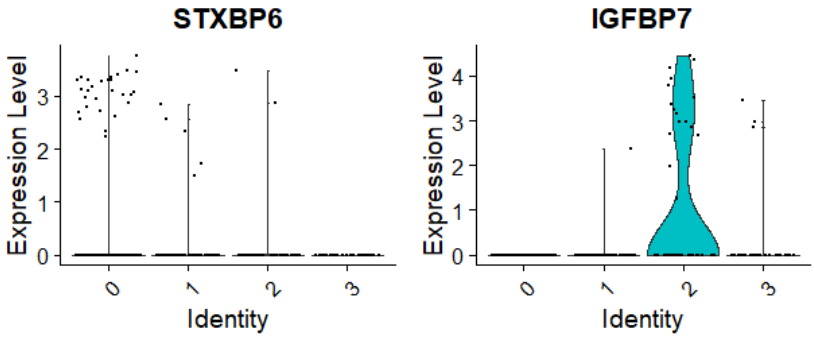

Fig. 9 Expression Pattern of ALS Reversal-Associated genes across Remyelinated MS ODC clusters visualized by Violin Plots (Cluster 2 expresses elevated levels of IGFBP7)

Next, I compared ALS Reversal-associated gene expression differences between MS patients experiencing plateaus and those without by screening the expression of IGFBP7 between remyelinated and demyelinated MS ODC populations. I isolated and pre-processed the demyelinated oligodendrocytes, and clustered the demyelinated ODC subgroup into 11 clusters, Next, I visualized the expression of ALS Reversal-associated genes across all demyelinated ODC MS clusters (**Fig. 10**).

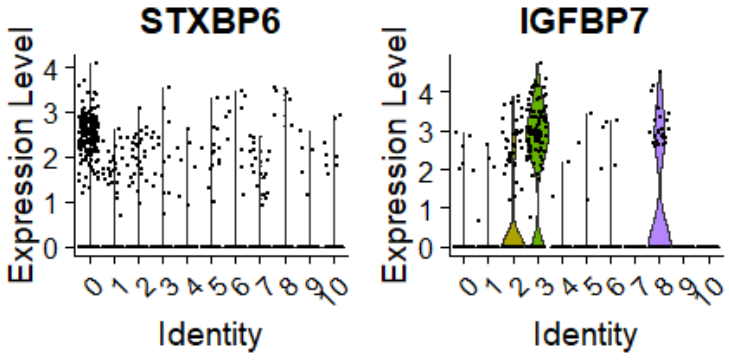

Fig. 10 Expression Pattern of ALS Reversal-associated genes across Demyelinated MS ODC clusters visualized by Violin Plots (Cluster 3 and 8 expresses elevated levels of IGFBP7)

Both remyelinated and demyelinated ODCs showed low expressions of STXBP6. On the other hand, cluster 2 in remyelinated ODC cells and 3 and 8 in demyelinated ODCs demonstrate marked elevated expression of IGFBP7. I hypothesized that these clusters with elevated IGFBP7 levels share the same cellular identity, and belong the same subtype of ODCs. Thus, to determine the cellular identity of these ODC clusters, I screened both the remyelinated and demyelinated clusters by an ODC subtype canonical marker list (SOX6, APOE, CDH20, CDH19, KLK6, OPALIN, KIRREL3 and ELL2) as provided by Jakel et al. (**Fig. 11**, **Fig. 12**).

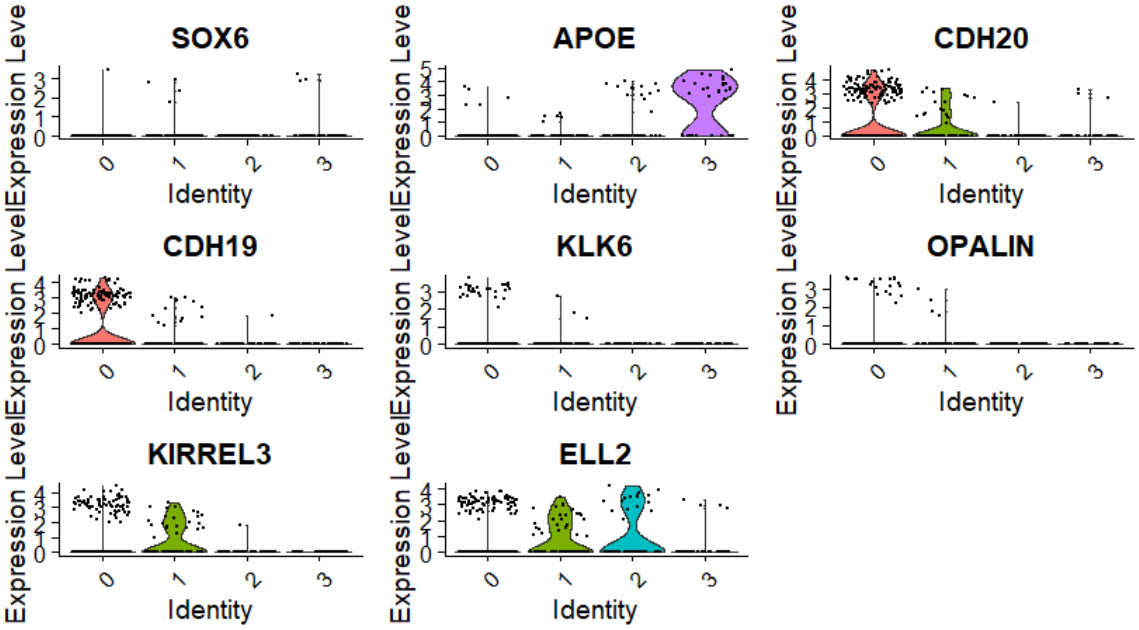

Fig. 11 Expression Pattern of ODC Subtype Canonical Markers across Remyelinated MS ODC clusters visualized by Violin Plot (Cluster 2, which expresses high levels of IGFBP7 in Figure 9, also express elevated levels of ELL2)

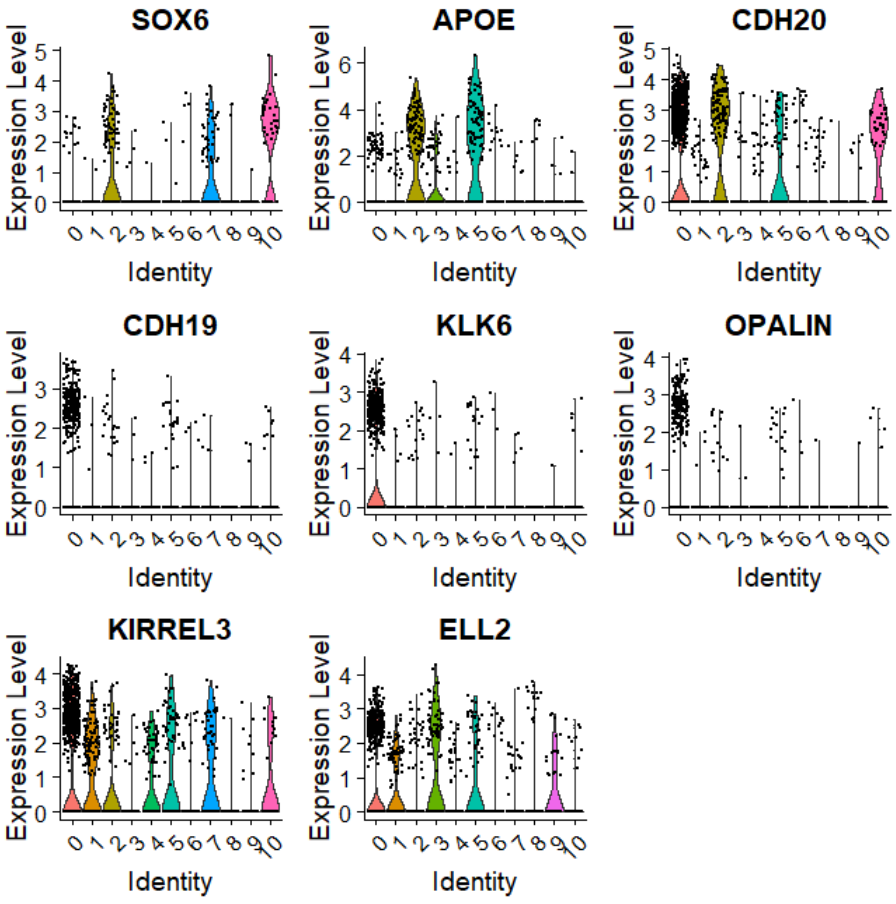

Fig. 12 Expression Pattern of ODC Subtype Canonical Markers across Demyelinated MS ODC clusters visualized by Violin Plot (Cluster 3, which expresses the highest levels of IGFBP7 across all demyelinated clusters in Figure 10, also express elevated levels of ELL2)

Clusters expressed elevated levels of IGFBP7 also expressed high levels of ELL2 in both remyelinated and demyelinated ODCs. According to original literature, ELL2 a canonical marker for an ODC subtype with wound healing and myelination properties [20]. Interestingly, IGFBP7 is also implicated in the stimulation of growth hormones (GH), leading to cell regeneration and neuronal development [29]. These results indicate that IGFBP7 may be involved in an ODC subtype-specific molecular pathway related to wound regeneration and remyelination.

I then asked if regular ODCs naturally expressed similar wound healing pathways. Hence, I compared ALS-associated gene expression levels of MS and regular spinal cord nuclei ODCs. I visualized the expression of ALS Reversal-associated genes across oligodendrocytes in Blum et al.'s spinal cord nuclei dataset (**Fig. 13**).

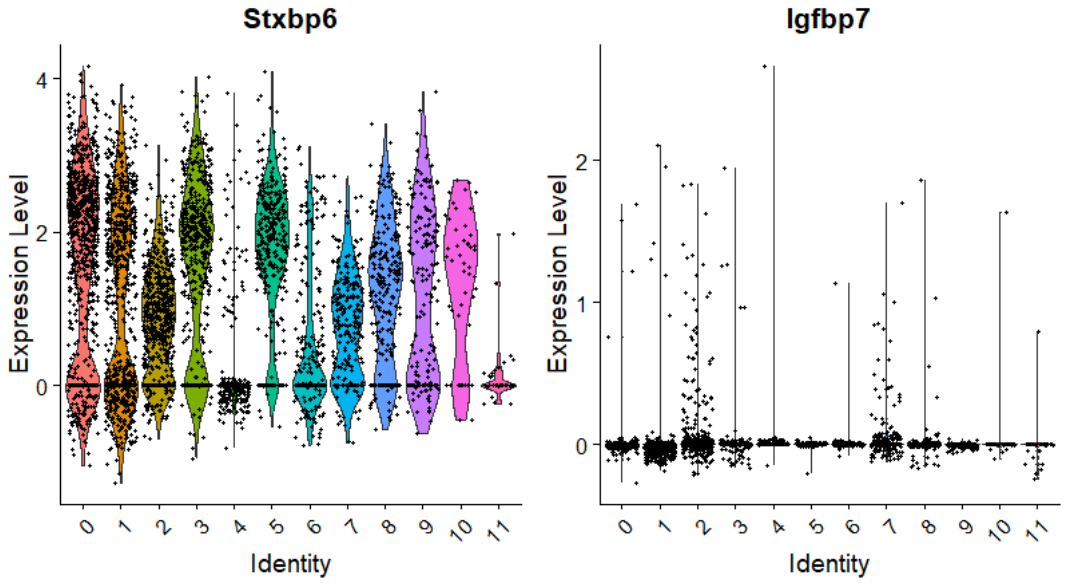

Fig. 13 Expression Pattern of ALS Reversal-associated genes across Demyelinated ODC clusters visualized by Violin Plots

ODCs in the spinal cord nuclei dataset show extremely low expressions of the gene IGFBP7 (**Fig. 13**), while all ODC populations in MS express significantly higher levels of IGFBP7 in selected clusters of ODCs. These results are striking, as they indicate that IGFBP7 specific pathways have not been activated in regular ODCs, while in MS ODCs IGFBP7 pathways are activated and contribute to remyelination. Thus, IGFBP7 may trigger mechanisms antagonizing ALS disease progression in an ODC-specific molecular pathway related to myelination and wound regeneration.

3.3. Effect of ALS Reversal pathway-inducing medication on C. elegans

My computational analysis indicates that IGFBP7 and STXBP6 potentially function in

distinct cell-type specific pathways, potentially mitigating ALS symptoms. Elevated levels IGFBP7 can be hypothesized to have a protective effect on oligodendrocytes of ALS Reversal patients, preventing demyelination during the ALS pathogenesis and effectively maintaining neuron integrity and survival. STXBP6 expresses elevated levels in α MN subtypes resistant to ALS degeneration, and may exert a protective effect on MNs.

My hypothesis posits that individual ALS Reversal-associated genes could specifically target and modulate ALS symptoms by upregulating distinct pathways. Thus, I ask the question if these two pathways exhibit synergistic effects with each other, to greater amplify their protective effect on ALS patients. I am able to test my hypothesis by upregulating ALS-gene associated autophagy and cell regeneration pathways in *C. elegans* SOD1 ALS models, and examining its effects on worm longevity and behavior.

I utilized *C. elegans*, a model well-recognized in ALS drug research, due to their simplicity and efficacy in assessing drug interventions for neurodegenerative diseases. They exhibit clear disease phenotypes, make them useful models for examining ALS symptom progression and drug effectiveness. Moreover, their short lifespan and easy maintenance provides me a perfect opportunity to test my hypothesis with limited time and resources.

I selected two drugs to simulate the impact of ALS Reversal-associated genes on the disease progression. To model the effects of STXBP6 acting on the autophagy pathway, I used Trehalose, an autophagy inducing drug currently undergoing phase 3 of clinical trials for ALS treatment. Trehalose has been shown to extend lifespan of ALS C. *elegans* models [30], and thus, worms administered with Trehalose will be used as a positive experimental control group. IGFBP7 regulates the levels of IGFs and enhances levels of IGF-1, resulting in activation of cell regeneration pathways. To model the effects of IGFBP7, I used Ibutamoren (MK677), a Ghrelin Receptor agonist that enhances the release of growth hormones and increases the levels of IGF-1 by acting on a molecular pathway similar to that of IGFBP7. By combining both drugs and measuring their protective effect on the survival of worms, we may be able to measure more pronounced ALS plateau, symptom rescue and even recovery on worm models. Such findings could offer crucial insights into potential therapeutic strategies and treatments for ALS patients.

3.3.1. Combinatorial Treatment of Trehalose & MK677 extends lifespan in SOD1 worm models

To assess the therapeutic potential of activating both ALS Reversal associated pathways, I compared lifespan in different groups to determine whether combinatorial treatment had

significant benefits on longevity of ALS worm models. Worms treated with Trehalose and MK677 respectively both had extended lifespans compared to control groups **(Fig. 14A**, P= 0.0446**)**, with lifespan extension in Trehalose treated groups being more significant (**Fig. 14B**, P = 0.0038). This is an expected result, as Trehalose has been shown to extend worm longevity and serves as a positive control in this experiment. These results demonstrate that MK677 and Trehalose independently activate cell pathways that exert protective effects on SOD1 G93A worm models.

Combined treatment of Trehalose & MK677 significantly prolonged the lifespan of SOD1 G93A worms compared to the control group (**Fig. 14A**, P = 0.002), with mean lifespan increasing from 7 to 12 days **(Fig. 14C)**. To confirm that lifespan extension of the combined treatment group is a result of both ALS Reversal-associated pathways acting together, and not the result of a single pathway, I compared the lifespan of Trehalose with the combined treatment. Although a Log-rank testing evaluating the significance of these two curves show to be relatively statistically insignificant (**Fig. 14B**, P = 0.1860), there is still an increased survival trend of worms treated with Trehalose and MK677 lifespan as compared to those treated with only Trehalose, demonstrated by the survival curve (**Fig. 14A**). These results indicate that autophagy pathways activated by Trehalose and cell regeneration pathways activated by MK677 have complementary effects on SOD1 G93A worm models, exerting neuroprotective effects and extending lifespan.

3.3.2. Combinatorial Treatment alleviates motor dysfunction in SOD1 worm models

To determine if ALS symptoms were slowed during activation of ALS Reversal-associated pathways, I performed locomotion assays on worms from all experimental conditions at age of 7, 9 and 11 days (**Fig. 15**). Across the span of these 5 days, the control group of SOD1 G93A transgenic worms (**Fig. 16A**) showed consistently low locomotor activity, demonstrating clear ALS disease phenotypes of paralysis and motor deficits. Worms treated with MK677 showed markedly high locomotion at day 7 (**Fig. 16B**), but MK677-treated worm movement quickly deteriorated as days progressed (**Fig. 16C**, **Fig. 16D**). Worms treated with Trehalose were not as active as those treated with MK677, but worm activity did not deteriorate as drastically as MK677 groups (**Fig. 16E**). Overall, both Trehalose and MK677 treated worm groups exhibited significantly higher locomotion than the control groups, indicating both drugs activated pathways that attenuates ALS motor deficits.

Worms administered with both Trehalose and MK677 showed clear improvements in motor function compared to the control group, and even the group treated with Trehalose (**Fig. 16B**)

(**Fig. 16C**). Locomotor behavior of combined treatment worms also stayed consistent throughout the 5-day assay (**Fig. 16E**), while other drug-treated worm condition groups' locomotion deteriorated significantly. This indicates upregulating both pathways exert greater, and more consistent protective effects on worm motor function, supporting my hypothesis of two pathways acting synergistically to alleviate ALS symptoms.

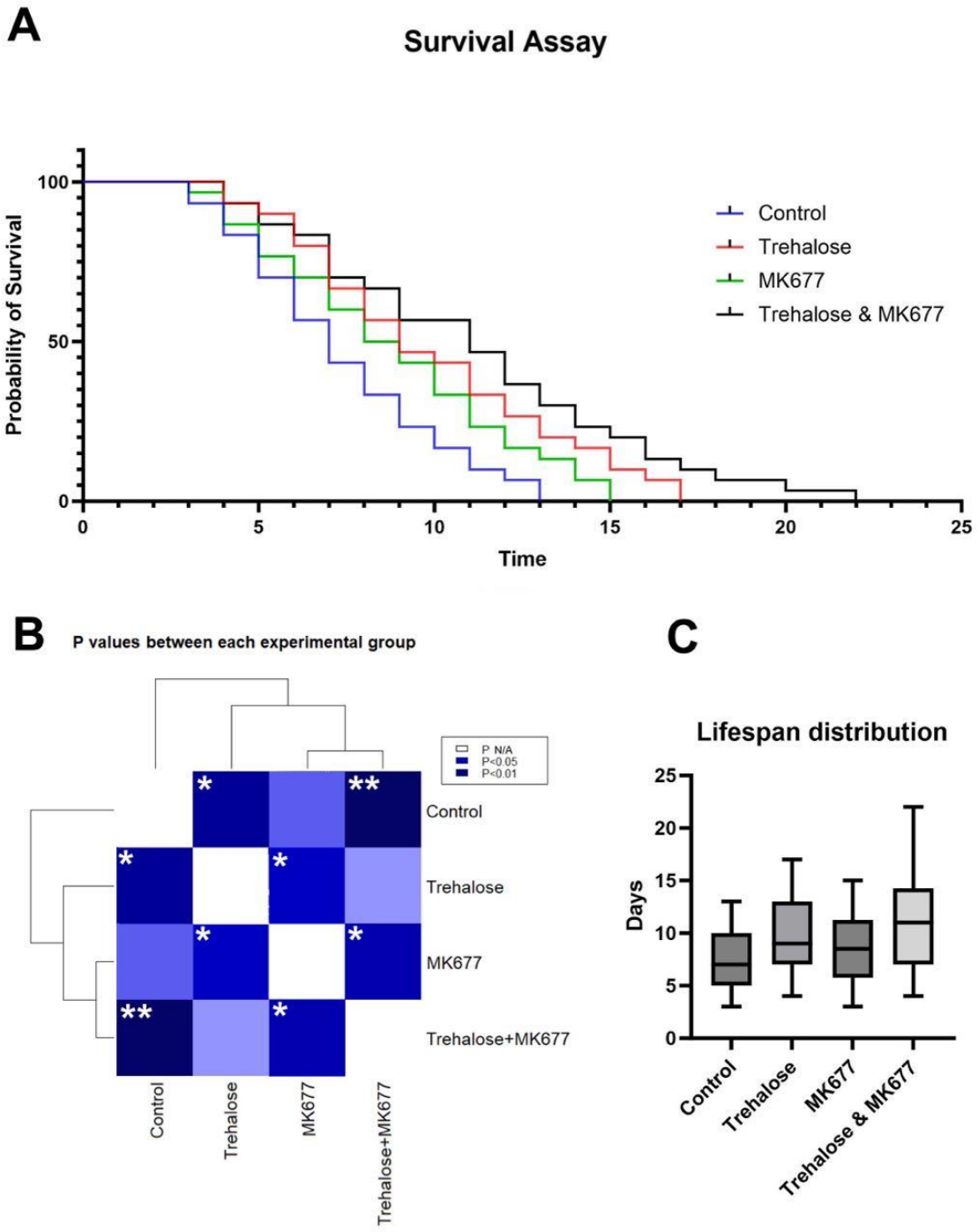

Fig. 14 Survival analysis of experiment groups. (A) Survival curve comparison of SOD1 G93A transgenic worms treated with Trehalose (n = 30), MK677 (n = 30), Trehalose & MK677 combined (n = 30) and control (n = 30). **(B)** Heatmap showing P values of each comparison, evaluated by Log-Rank (Mantel-Cox) Test. **(C)** Bar graph of median lifespan across all worm conditions. **P<0.01; *P<0.05

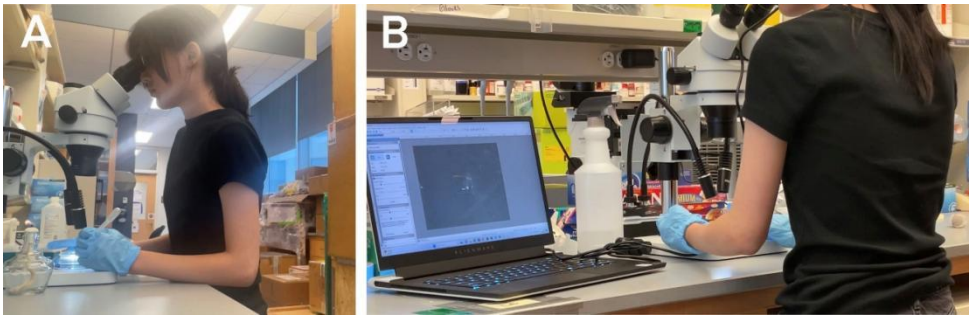

Fig. 15 Assays of SOD1 G93A *C. elegans.* (A) Survival Assay of *C. elegans.* **(B)** Locomotion Assay of *C. elegans.*

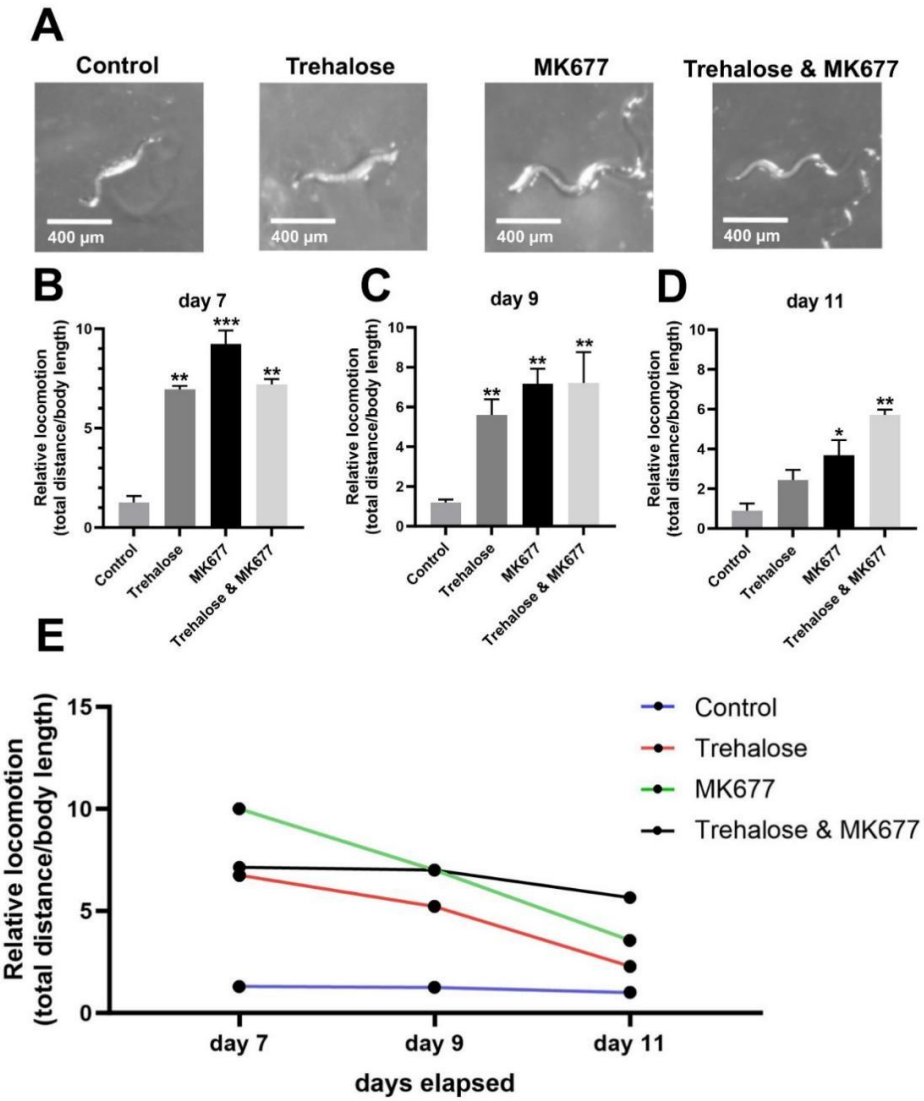

Fig. 16 Locomotion Assay of SOD1 G93A *C. elegans* Experiment Groups. **(A)** Locomotion Assay of representative worm across all conditions at age of day 7. **(B)** Bar graph of relative locomotion of all worm conditions at day 7 (n = 3 for each experimental group). **(C)** Bar graph of relative locomotion of all worm conditions at day 9 (n = 3 for each experimental group). **(D)** Bar graph of relative locomotion of all worm conditions at day 11(n = 3 for each experimental group). **(E)** Line graph of relative locomotion of all worm conditions at days 7, 9 and 11; each data point represents relative locomotion of one condition at a given day. ***P < 0.001; **P < 0.01; *P<0.05, each comparison was performed between the experimental group and control.

4. Discussion

In summary, my findings from cell-type identification and ALS Reversal gene screening of snRNA and scRNA sequencing data revealed two ODC and MN cell-specific pathways associated with ALS Reversal cases. Analysis of MS ODC subtype identities reveals this ODC cell-specific pathway might ameliorate ALS symptoms through myelination, wound repair and regeneration. Notably, further investigation of the MN-specific pathway indicated an association between ALS Reversals and autophagy, suggesting that upregulation of autophagy pathways may exert protective effects on MNs and conserve motor function in ALS patients. Furthermore, I tested my hypothesis with *C. elegans* models, which demonstrates upregulated ALS Reversal-associated pathways improve motor function and extends lifespan in SOD1 ALS models. These results support my hypothesis that mechanisms behind ALS Reversals involve synergistic cross-talk between autophagy and remyelination pathways. These upregulated pathways ameliorate and plateau ALS symptoms, extend longevity, and could potentially trigger functional recovery.

My research opens up many future points for discussion. First of all, one potential caveat of this study is that cases of ALS Reversal cases are very rare, and serve as outliers to the general ALS population [10]. Hence, why should we study these outliers? Although some ALS patients, famously including the theoretical physicist Stephen Hawking, can live long periods with diagnosed ALS, for most ALS populations, disease progression is swift, fatal and mostly irreversible. However, there is still value in studying exceptions: as they can potentially provide us insightful directions towards disease recovery. An example of outliers paving the way for therapeutic breakthroughs in disease is in HIV research. Two famous HIV functional recovery cases, the ‘Berlin Patient’ and ‘London Patient’ [31], inspired extensive research and led to the success of antiretroviral therapy (ART) as functional lifelong treatment for HIV patients [32]. Moreover, examining HIV patients who control virus replication independent of ART therapy (‘elite controllers’) has led to promising new directions of HIV functional treatment [33]. Thus, when evaluating the significance of outliers in the context of ALS, we should take care to eliminate noise and extract useful data. For instance, one study highlighted that ALS Reversal patients had a higher likelihood of being in professions related to woodworking compared to the general ALS patient population [12]. Future researchers may test the significance of this difference by investigating the molecular specific ways chemical exposures in these professions impact ALS pathogenesis.

Secondly, due to the limitations of high school students to perform experiments on mammalian models, it is not feasible for me to validate the therapeutic effect on SOD1 mouse (*Mus musculus*) models. Admittedly, complex animal models may provide insights into ALS disease pathology that cannot be produced in simpler organisms. However, simple animal models offer unique advantages that make them invaluable for uncovering insights in ALS pathogenesis. *C. elegans* and fruit flies (*Drosophila melanogaster*) have well-studied and documented nervous systems and stress pathways [35], and offer readily available, efficient methods to manipulate protein expression in a range of cell types [35]. Using *C. elegans* and *D. melanogaster* models also allows me to examine other ALS gene mutations, such as C9orf72 and TDP-43. This makes them ideal models to examine mechanisms of neuronal toxicity in neurodegenerative diseases. Yeast models have also led to prominent discoveries in ALS – researchers first uncovered the importance of TDP-43 protein misfolding in ALS progression using budding yeast [36]. Hence, my experimentation on *C. elegans* offers valid results and meaningful discoveries, and I invite future researchers to confirm my findings with more complex mammalian models.

Finally, my research provides new directions in the field of ALS therapy and clinical recovery. In my paper, I have hypothesized two pathways of ALS Reversal mechanisms, which may provide insights in recreating ALS symptom amelioration and functional recovery. The beneficial effects of combinatorial treatment of Trehalose and MK677 in my research also draws interesting parallels to other approved drugs for ALS. AMX0035, an FDA-approved drug, is also a combinatorial therapy medication consisting of sodium phenylbutyrate and taurursodiol [37]. The medication has demonstrated survival and functional benefits in ALS in Phase-3 trials [38]. The mechanisms underlying combinatorial treatment may also link to the heterogeneity of ALS pathogenesis. On a molecular level, MN death in ALS is likely a result of multifactorial influences [39], and combinatorial treatments may exert protective effects in multiple pathways, resulting in enhanced protection of MNs and prolonged functionality. Thus, examining the effects of activating synergistic pathways in ALS treatment could offer potential directions for therapeutic treatment, and provide insight on how to replicate these reversal miracles on larger ALS populations.

References

[1] Masrori P, Van Damme P. Amyotrophic lateral sclerosis: a clinical review. Eur J Neurol. 2020 Oct;27(10):1918-1929.

[2] Chiò A, Logroscino G, Traynor BJ, Collins J, Simeone JC, Goldstein LA, White LA. Global epidemiology of amyotrophic lateral sclerosis: a systematic review of the published literature. Neuroepidemiology. 2013;41(2):118-30.

[3] Arthur KC, Calvo A, Price TR, Geiger JT, Chiò A, Traynor BJ. Projected increase in amyotrophic lateral sclerosis from 2015 to 2040. Nat Commun. 2016 Aug 11;7:12408.

[4] Rowland, L. P. & Shneider, N. A. Amyotrophic lateral sclerosis. N. Engl. J. Med. 344, 1688–1700 (2001).

[5] Hinchcliffe M, Smith A. Riluzole: real-world evidence supports significant extension of median survival times in patients with amyotrophic lateral sclerosis. Degener Neurol Neuromuscul Dis. 2017 May 29;7:61-70.

[6] Paganoni S, Hendrix S, Dickson SP. Long-term survival of participants in the CENTAUR trial of sodium phenylbutyrate-taurursodiol in amyotrophic lateral sclerosis. Muscle Nerve. 2021 Jan;63(1):31-39.

[7] Tucker T, Layzer RB, Miller RG, Chad D. Subacute, reversible motor neuron disease. Neurology. 1991 Oct;41(10):1541-4.

[8] Bedlack RS, Vaughan T, Wicks P, Heywood J, Sinani E, Selsov R, Macklin EA, Schoenfeld D, Cudkowicz M, Sherman A. How common are ALS plateaus and reversals? Neurology. 2016 Mar 1;86(9):808-12.

[9] Cedarbaum JM, Stambler N, Malta E, Fuller C, Hilt D, Thurmond B, Nakanishi A. The ALSFRS-R: a revised ALS functional rating scale that incorporates assessments of respiratory function. BDNF ALS Study Group (Phase III). J Neurol Sci. 1999 Oct 31;169(1-2):13-21.

[10] J. Crayle, M. Lutz, J. Raymond, P. Mehta & R. Bedlack (2023) Study of "ALS reversals": LifeTime environmental exposures (StARLiTE), Amyotrophic Lateral Sclerosis and Frontotemporal Degeneration, 24:1-2, 54-62.

[11] Duke University, study of ALS Reversals 2: Genetic Analyses (StAR2)

[12] Bedlack RS, Everything ALS. (2022, November 27). *Richard Bedlack on ALS Reversals: An Update for 2022* [Video].

[13] Raffaele S, Boccazzi M, Fumagalli M. Oligodendrocyte Dysfunction in Amyotrophic Lateral Sclerosis: Mechanisms and Therapeutic Perspectives. Cells. 2021 Mar 5;10(3):565.

[14] Lubetzki C, Zalc B, Williams A, Stadelmann C, Stankoff B. Remyelination in multiple sclerosis: from basic science to clinical translation. Lancet Neurol. 2020 Aug;19(8):678-688.

[15] Blum, J.A., Klemm, S., Shadrach, J.L. *et al.* Single-cell transcriptomic analysis of the adult mouse spinal cord reveals molecular diversity of autonomic and skeletal motor neurons.*Nat Neurosci* **24**, 572–583 (2021).

[16] Satija, R., Farrell, J., Gennert, D. *et al.* Spatial reconstruction of single-cell gene expression data. *Nat Biotechnol* 33, 495–502 (2015).

[17] Jolliffe Ian T. and Cadima George, 2016 Principal component analysis: a review and recent developments*Phil. Trans. R. Soc. A.*3742015020220150202.

[18] Seth S, Mallik S, Bhadra T and Zhao Z (2022) Dimensionality Reduction and Louvain Agglomerative Hierarchical Clustering for Cluster-Specified Frequent Biomarker Discovery in Single-Cell Sequencing Data. *Front. Genet.* 13:828479

[19] McInnes, Leland, John Healy, and James Melville. "Umap: Uniform manifold approximation and projection for dimension reduction." *arXiv preprint arXiv:1802.03426* (2018).

[20] Jäkel S, Agirre E, Mendanha Falcão A, van Bruggen D, Lee KW, Knuesel I, Malhotra D, French-Constant C, Williams A, Castelo-Branco G. Altered human oligodendrocyte heterogeneity in multiple sclerosis. Nature. 2019 Feb;566(7745):543-547.

[21] Castro Torres T, Moaddeli D, Averbukh M, Coakley AJ, Dutta N, Garcia G, Higuchi-Sanabria R. Surveying Low-Cost Methods to Measure Lifespan and Healthspan in Caenorhabditis elegans. J Vis Exp. 2022 May 18;(183):10.3791/64091.

[22] Wang J, Farr GW, Hall DH, Li F, Furtak K, Dreier L, Horwich AL, An ALS-linked mutant SOD1 produces a locomotor defect associated with aggregation and synaptic dysfunction when expressed in neurons of Caenorhabditis elegans, PLoS Genet. 5 (1) (2009), e1000350.

[23] Ragagnin AMG, Shadfar S, Vidal M, Jamali MS and Atkin JD (2019) Motor Neuron Susceptibility in ALS/FTD. *Front. Neurosci.* 13:532

[24] Lenka G, Shan J, Halabi N, Abuaqel SWJ, Goswami N, Schmidt F, Zaghlool S, Romero AR, Subramanian M, Boujassoum S, Al-Bozom I, Gehani S, Khori NA, Bedognetti D, Suhre K, Ma X, Dömling A, Rafii A, Chouchane L. STXBP6, reciprocally regulated with autophagy, reduces triple negative breast cancer aggressiveness. Clin Transl Med. 2020 Aug 11;10(3):e147.

[25] Chua JP, De Calbiac H, Kabashi E, Barmada SJ. Autophagy and ALS: mechanistic insights and therapeutic implications. Autophagy. 2022 Feb;18(2):254-282.

[26] Sasaki S. Autophagy in spinal cord motor neurons in sporadic amyotrophic lateral sclerosis. J Neuropathol Exp Neurol. 2011 May;70(5):349-59.

[27] Bordi, M., De Cegli, R., Testa, B. *et al.* A gene toolbox for monitoring autophagy transcription. *Cell Death Dis* 12, 1044 (2021).

[28] Trojsi F, Sagnelli A, Cirillo G, Piccirillo G, Femiano C, Izzo F, Monsurrò MR, Tedeschi G. Amyotrophic lateral sclerosis and multiple sclerosis overlap: a case report. Case Rep Med. 2012; 2012:324685.

[29] Hwa V, Oh Y, Rosenfeld RG. The insulin-like growth factor-binding protein (IGFBP) superfamily. Endocr Rev. 1999 Dec;20(6):761-87.

[30] Honda Y, Tanaka M, Honda S. Trehalose extends longevity in the nematode Caenorhabditis elegans. Aging Cell. 2010 Aug;9(4):558-69.

[31] Ding J, Liu Y, Lai Y. Knowledge From London and Berlin: Finding Threads to a Functional HIV Cure. Front Immunol. 2021 May 27;12:688747.

[32] Bailon L, Mothe B, Berman L, Brander C. Novel Approaches Towards a Functional Cure of HIV/AIDS. Drugs. 2020 Jun;80(9):859-868.

[33] Gebara NY, El Kamari V, Rizk N. HIV-1 elite controllers: an immunovirological review and clinical perspectives. J Virus Erad. 2019 Sep 18;5(3):163-166.

[34] Hegde KN, Srivastava A. *Drosophila melanogaster* as a Tool for Amyotrophic Lateral Sclerosis Research. J Dev Biol. 2022 Aug 30;10(3):36.

[35] Casci I, Pandey UB. A fruitful endeavor: modeling ALS in the fruit fly. Brain Res. 2015 May 14;1607:47-74.

[36] Armakola M, Hart MP, Gitler AD. TDP-43 toxicity in yeast. Methods. 2011 Mar;53(3):238-45.

[37] Qingyang Xu, Joonhyuk Cho, Zied Ben Chaouch & Andrew W. Lo (2023) Incorporating patient preferences and burden-of-disease in evaluating ALS drug candidate AMX0035: a Bayesian decision analysis perspective, Amyotrophic Lateral Sclerosis and Frontotemporal Degeneration, 24:3-4, 281-288.

[38] Paganoni S, Hendrix S, Dickson SP, Knowlton N, Macklin EA, Berry JD, Elliott MA, Maiser S, Karam C, Caress JB, Owegi MA, Quick A, Wymer J, Goutman SA, Heitzman D, Heiman-Patterson TD, Jackson CE, Quinn C, Rothstein JD, Kasarskis EJ, Katz J, Jenkins L, Ladha S, Miller TM, Scelsa SN, Vu TH, Fournier CN, Glass JD, Johnson KM, Swenson A, Goyal NA, Pattee GL, Andres PL, Babu S, Chase M, Dagostino D, Hall M, Kittle G, Eydinov M, McGovern M, Ostrow J, Pothier L, Randall R, Shefner JM, Sherman AV, St Pierre ME, Tustison E, Vigneswaran P, Walker J, Yu H, Chan J, Wittes J, Yu ZF,

Cohen J, Klee J, Leslie K, Tanzi RE, Gilbert W, Yeramian PD, Schoenfeld D, Cudkowicz ME. Long-term survival of participants in the CENTAUR trial of sodium phenylbutyrate-taurursodiol in amyotrophic lateral sclerosis. Muscle Nerve. 2021 Jan;63(1):31-39.

[39] Beghi E, Mennini T, Bendotti C, Bigini P, Logroscino G, Chiò A, Hardiman O, Mitchell D, Swingler R, Traynor BJ, Al-Chalabi A. The heterogeneity of amyotrophic lateral sclerosis: a possible explanation of treatment failure. Curr Med Chem. 2007;14(30):3185-200.

Acknowledgements

Although all bioinformatic analysis and wet lab procedures were performed by myself, I would like to thank Keyuan Ren, Eva Wang, Douglas Jiang, Dr. Hong Guo, Ray Jiang, Isha Nagireddy and Dr. Feng Tian from Beth Israel Deaconess Medical Center (BIDMC) and Harvard Medical School (HMS) during the completion of my research project for their help and guidance. I would also like to thank Mr. Jason Wilson, for suggesting this project and giving me helpful advice throughout. Finally, I am grateful to my parents for their continued support and encouragement.

Declaration of Academic integrity

The author declares no conflict of interest.

The project was completed at BIDMC and HMS, where the student was enrolled as an internship student. The student affirms that BIDMC and HMS have full legal rights and ownership over any potential intellectual property generated in this study. Any unauthorized use, reproduction, distribution, modification, or disclosure of the aforementioned intellectual property, in part or in whole, without the explicit written consent by BIDMC and HMS, shall constitute infringement under the applicable laws and may result in legal action. No domestic or international collaboration has been established based on this project.

Supplementary Data

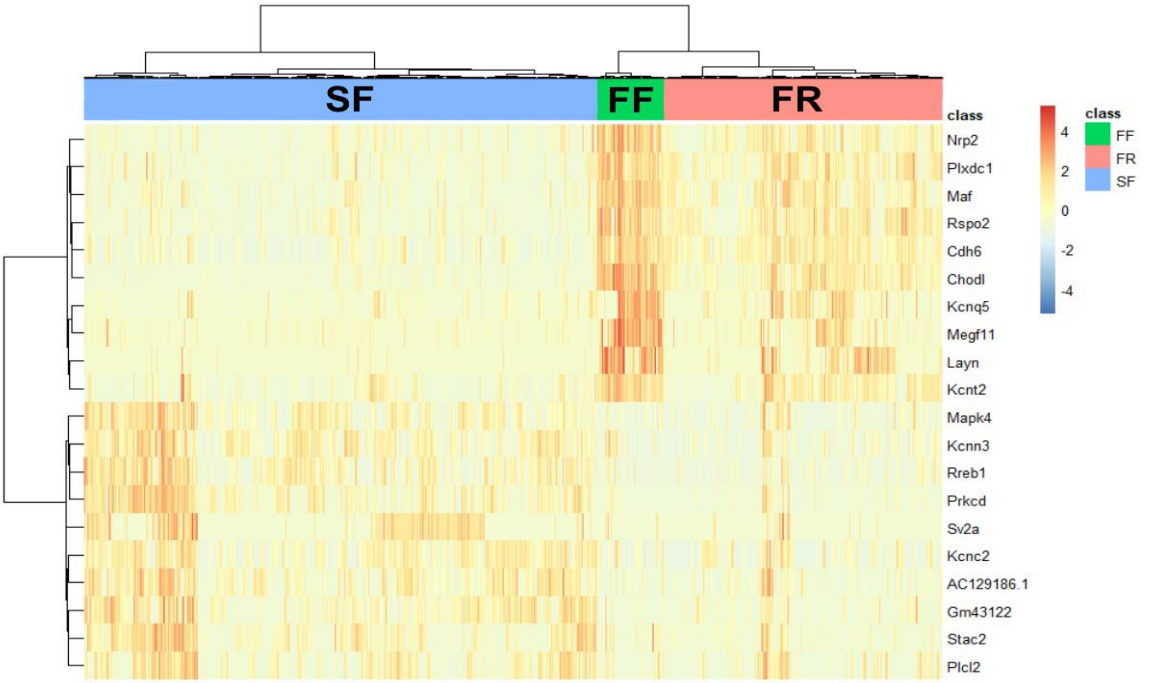

Supplementary Fig.1 Heat map showing all α MNs, colored by expression of differentially expressed marker genes for FF (fast firing) , SF (slow firing) , FR (fast fatigue-resistant)

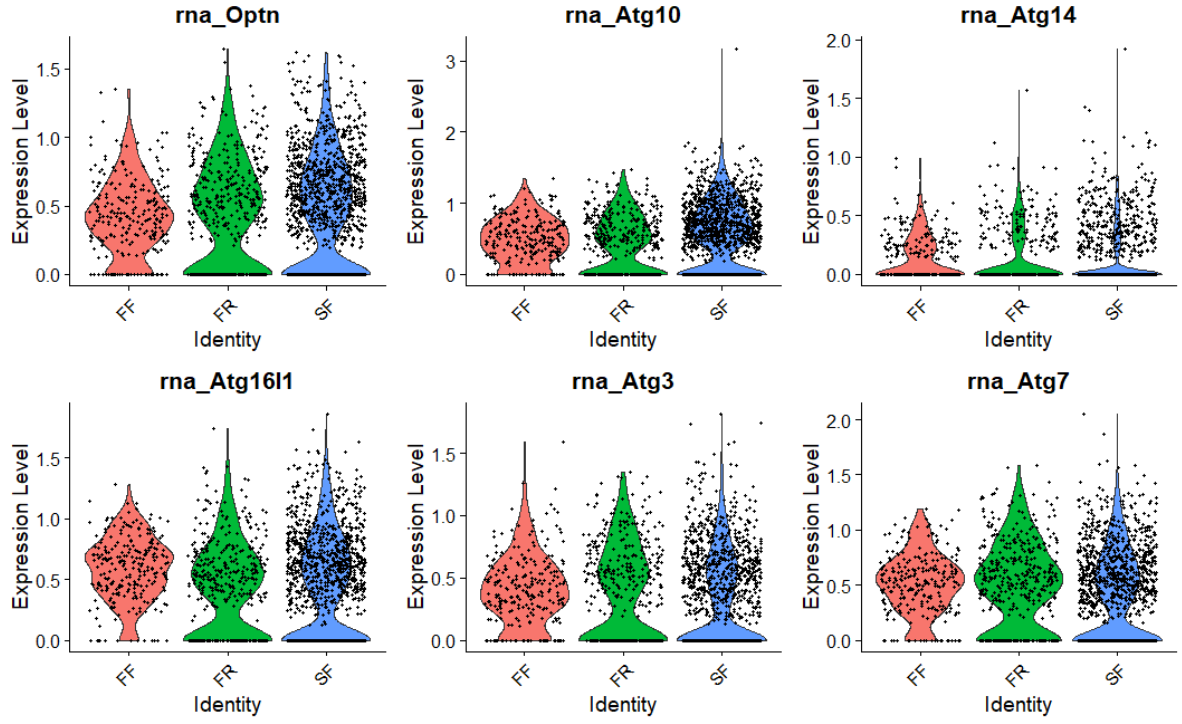

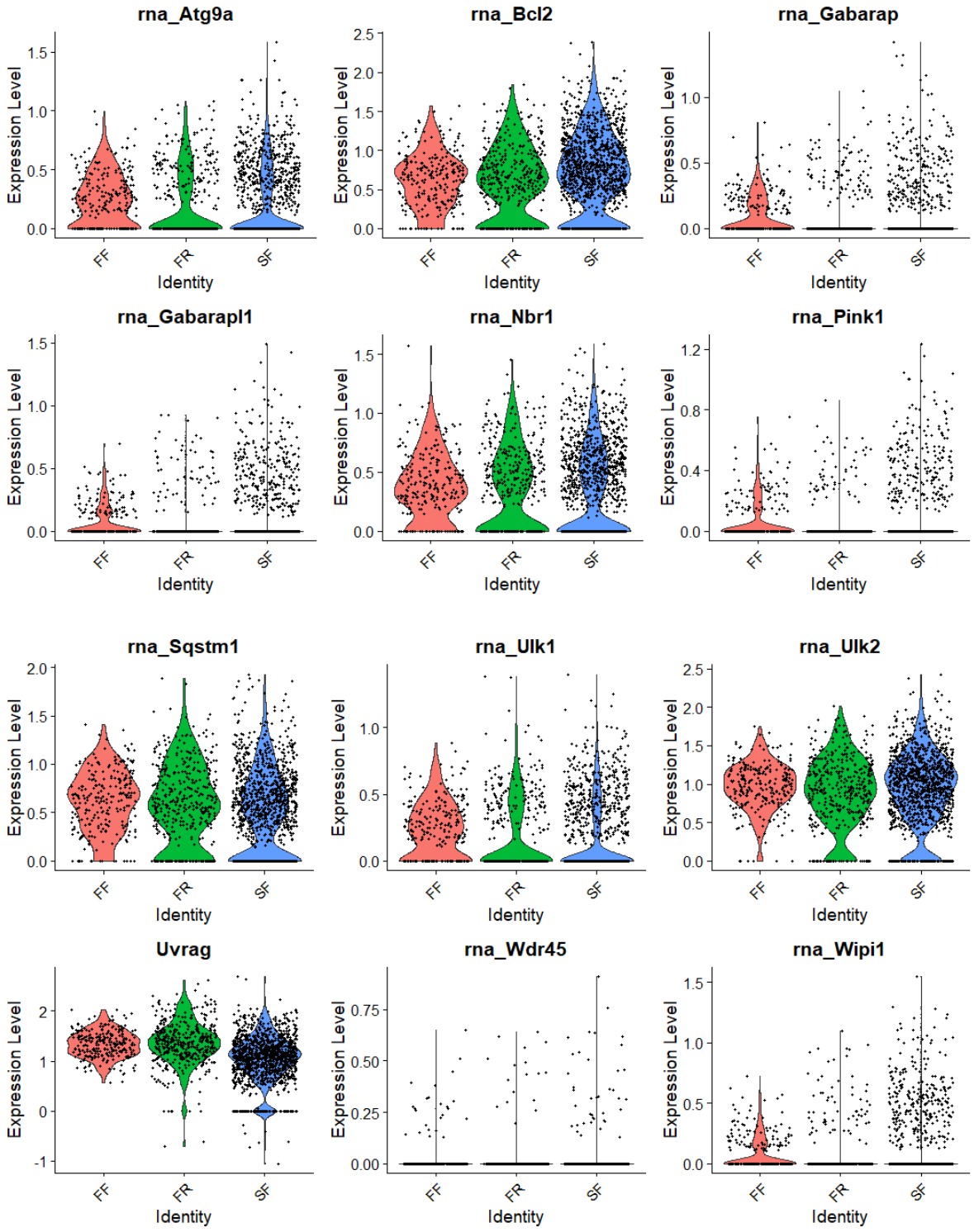

Supplementary Fig. 2 Expression Pattern of Autophagy Associated genes across α MN subtypes